

# The x-ray light valve: a low-cost, digital radiographic imaging system-spatial resolution

Robert D. MacDougall, Ivaylo Koprinarov, Christie Ann Webster and J.A. Rowlands  
Sunnybrook Health Sciences Centre, Department of Medical Biophysics, University of Toronto,  
2075 Bayview Ave., Toronto, Ontario, Canada M4N 3M5

## ABSTRACT

In recent years, new x-ray radiographic systems based on large area flat panel technology have revolutionized our capability to produce digital x-ray radiographic images. However, these active matrix flat panel imagers (AMFPIs) are extraordinarily expensive compared to the systems they are replacing. Thus there is a need for a low cost digital imaging system for general applications in radiology. Different approaches have been considered to make lower cost, integrated x-ray imaging devices for digital radiography, including: scanned projection x-ray, an integrated approach based on computed radiography technology and optically demagnified x-ray screen/CCD systems. These approaches suffer from either high cost or high mechanical complexity and do not have the image quality of AMFPIs. We have identified a new approach – the X-ray Light Valve (XLV). The XLV has the potential to achieve the immediate readout in an integrated system with image quality comparable to AMFPIs. The XLV concept combines three well-established and hence low-cost technologies: an amorphous selenium (*a*-Se) layer to convert x-rays to image charge, a liquid crystal (LC) cell as an analog display, and an optical scanner for image digitization. Here we investigate the spatial resolution possible with XLV systems. Both *a*-Se and LC cells have both been shown separately to have inherently very high spatial resolution. Due to the close electrostatic coupling in the XLV, it can be expected that the spatial resolution of this system will also be very high. A prototype XLV was made and a typical office scanner was used for image digitization. The Modulation Transfer Function was measured and the limiting factor was seen to be the optical scanner. However, even with this limitation the XLV system is able to meet or exceed the resolution requirements for chest radiography.

**Keywords:** Digital radiography DR, Direct conversion detectors, Digital x ray imaging radiography DX, Detector technology DET, X-ray light valve (XLV)

## 1. INTRODUCTION

The advantages of digital radiography over traditional film-screen radiography are well known<sup>1</sup> and it is has been established that a fully digital radiology department is desirable for all radiographic applications. Existing digital radiographic imaging systems are either prohibitively expensive and can only be used in a few exceptional institutions or suffer from poor image quality. The current leading technology is based on large area active matrix flat panel imagers (AMFPIs)<sup>2</sup>. While these AMFPIs provide increased functionality over standard film-screen cassette detectors, they are extraordinarily expensive and are therefore not seen as a feasible replacement to film-screen systems for general radiography. Other imaging systems such as cassette-based Computed Radiography (CR) detectors offer a more economic solution but at the cost of inferior image quality and higher dose to the patient<sup>3</sup>. CR systems are also much less convenient due to the need for moving cassettes from the x-ray room to a processing station. Other integrated approaches include scanned projection x-ray<sup>2</sup>, *a*-Se detector readout systems based on electrophotography<sup>4</sup>, and optically demagnified x-ray screen/camera systems<sup>5</sup>, as well as integrated systems based on CR technology. All suffer from the trade-off between image quality and cost or mechanical complexity<sup>6</sup>. Thus there is a need for a low-cost x-ray imaging system for general radiography which maintains or exceeds the image quality of AMFPIs without an increase in radiation dose.

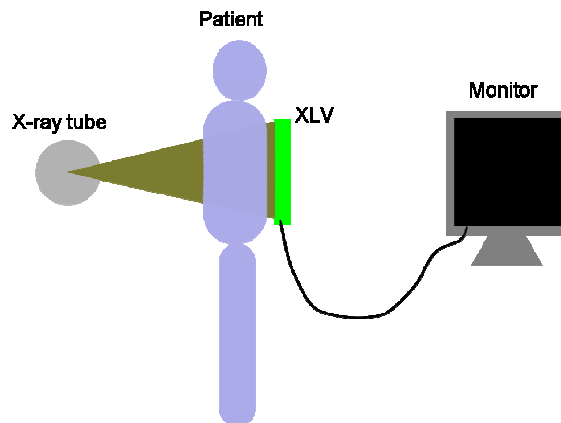


**Figure 1:** Integrated readout digital chest radiographic imaging system based on the XLV. X-rays produced in the x-ray tube are detected by an XLV detector. The image formed in the XLV detector is then digitized with an optical scanner and the image is ready for viewing at a nearby workstation.

We have identified a promising approach, the X-ray Light Valve (XLV)<sup>7,8</sup>, to address this need. The XLV is a fully integrated digital radiographic system as shown in Figure 1. It is based on three low-cost technologies: (i) amorphous selenium (*a*-Se) as an x-ray to charge transducer, (ii) a Liquid Crystal (LC) cell as an analog image display and (iii) an optical scanner for image digitization. The operation of the XLV system involves: exposure, optical image formation, image digitization, and reset. Each step is briefly described to provide a foundation for a discussion of system performance and spatial resolution to follow.

Figure 2a shows the components of the XLV detector in its rested state. The XLV detector is composed of top and bottom electrodes, an *a*-Se photoconductive layer and an LC cell. This LC cell is made of rod-like LC molecules which possess an optical anisotropy and an electrical polarizability. In its rested state, these LC molecules are aligned parallel to one another.

To acquire an x-ray image, an electric potential is applied to the top and bottom electrodes which creates an electric field  $E$  across the entire structure (Figure 2b). This causes the LC molecules to align with  $E$ . When an x-ray is absorbed in the *a*-Se layer, electron-hole pairs (ehp) are released and are guided by  $E$  to opposite surfaces of the *a*-Se layer. This ensures that there is very little lateral spread of charge and thus minimal blur in the charge image at the *a*-Se - LC interface and *a*-Se has been shown to have inherently high spatial resolution<sup>9,10</sup>. After the x-ray exposure, the large bias electric field applied via the bias electrodes can be removed.

The next step is the creation of an optically visible analog image in the LC cell. The charge trapped at the *a*-Se - LC interface creates a local  $E$  across the LC cell causing the adjacent LC molecules to align with it (Figure 2c). In regions where no charge has been accumulated, the LC molecules return to their rested state. By placing a linear polarizer on top of the LC cell and by choosing the appropriate thickness of the LC layer, the LC cell acts as a half-wave retarder when  $E=0$ . This means that incident light reflected off the *a*-Se surface will not escape the LC cell (Figure 2d(i)). Under high  $E$ , the LC molecules will align in the vertical direction such that all incident light will be reflected and escape the LC cell (Figure 2d(ii)). In this way, regions in the LC cell can be made to reflect light depending on the amount of image charge accumulated at the LC surface. Thus, an optically visible image is created in the LC cell which faithfully reproduces the absorbed x-ray energy pattern.

To store the image on a hard disk, an external light source and optical scanner are used for image digitization. The wavelength of the readout light is chosen so that it will not erase the image at the *a*-Se - LC interface. The image is scanned line by line over the entire XLV detector to form a digital radiograph.

A key feature of the XLV is that the charge image is stable at the *a*-Se - LC interface, allowing the readout to continue over minutes if desired. Following readout, the charge image has to be removed or erased before a fresh exposure is made. To do this, the photoconductor is flooded with actinic (i.e. optical radiation which frees ehp in the *a*-Se layer)

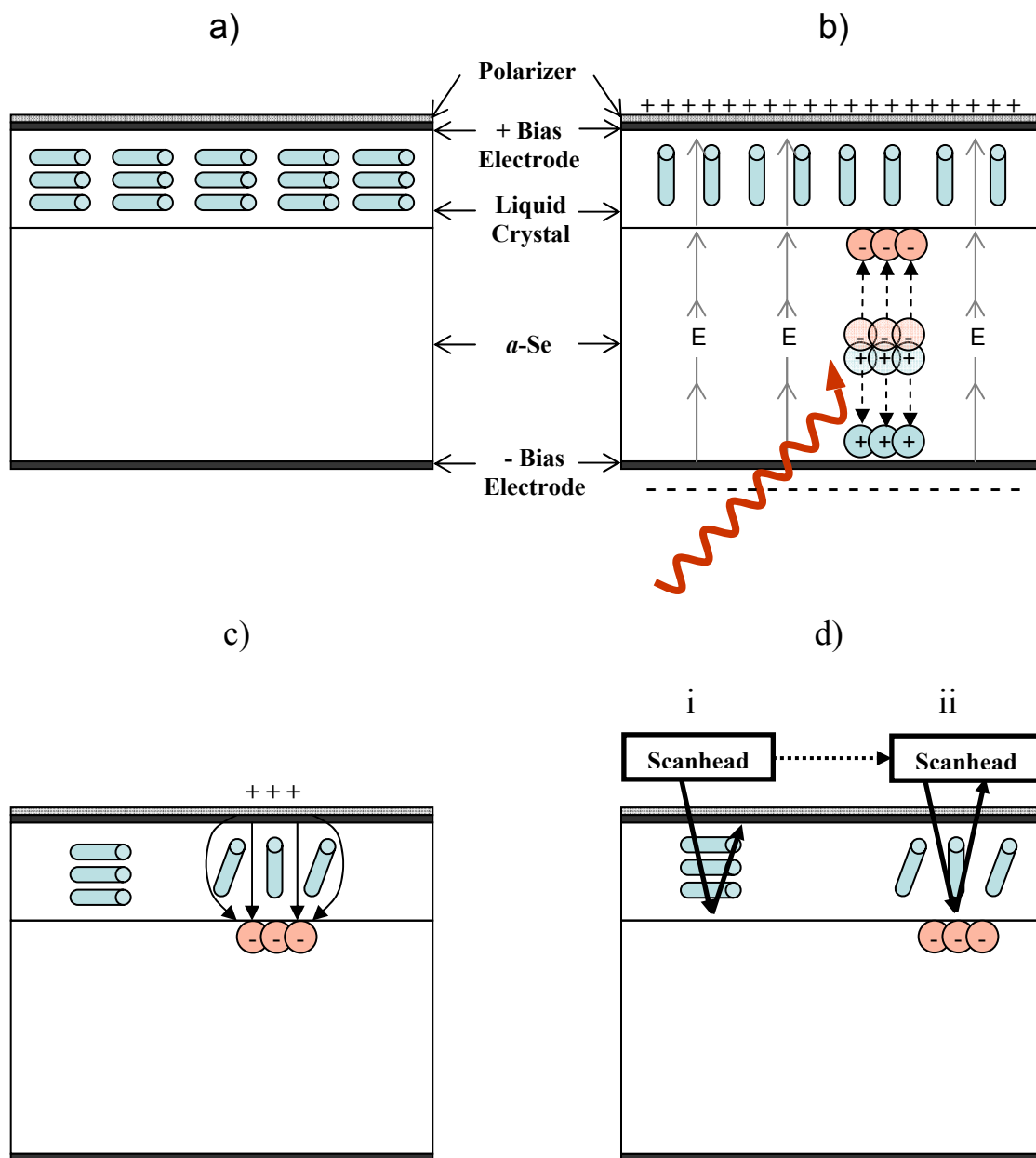


**Figure 2:** Process of image formation and digitization in the XLV: a) XLV in rested state prior to exposure, b) exposure: x-ray releases ehp in photoconductor which are guided to the *a*-Se – LC interface c) optical image formation: charges collected at interface form electric field across LC layer causing LC molecules to align with it creating an optically visible image, d) image digitization: an external light source shines light on the LC cell which is reflected off the *a*-Se surface and detected by a light diode where the LC molecules are aligned with *E*. Where the LC molecules are in the rested state, light is blocked by the polarizer and is not detected by the scanner.

light from white LEDs. The charges produced move so as to neutralize the remaining image charge and the LC molecules return to their rested state. The XLV is then ready to acquire a new image.

We have theoretically analyzed the properties of the XLV<sup>8</sup> and have shown its potential to meet clinical radiography requirements in terms of: x-ray quantum noise limited operation, high x-ray sensitivity, and adequate contrast over the exposure range of interest. The XLV exhibits low noise and x-ray quantum noise limited operation because it requires no external electronics. The fundamental sources of noise and the quantum efficiency of the proposed system have also been modeled<sup>7,8</sup>. It has been shown that by proper choice of the XLV design and operating parameters, x-ray exposures within the clinical exposure range can be optimized for desired imaging tasks<sup>8</sup>.

The spatial resolution of the XLV is expected to be high due to the design of the detector and the physics involved in image formation. The XLV device itself is not pixilated so that the resolution of the x-ray detector is governed by the physics of the x-ray to charge conversion, charge collection, field spreading and LC response. The complete system response will also include image digitization and the optical coupling of the XLV device to the pixilated optical readout array. Amorphous selenium has previously been demonstrated to have inherently high spatial resolution because in an electrostatic detector the image charge is guided by an electric field and moves directly to the surface resulting in minimal blur<sup>9,10</sup>. The LC cell is very thin and inherently has a resolution on the order of a few microns. Therefore, it is anticipated that high image resolution can be achieved with photodetector layers thick enough to provide high quantum efficiency. Here we will examine the resolution actually achievable in a practical implementation of an XLV.

## 2. MATERIALS

### 2.1. XLV Construction

An XLV was constructed for the purpose of measuring the MTF of the XLV system. The device consisted of a photoconductive *a*-Se layer and an LC cell in a sandwich structure. The bottom layer consisted of a 150  $\mu\text{m}$  *a*-Se plate evaporated onto an aluminum substrate which served as the bottom (negative) bias electrode. The top layer consisted of a transparent piece of glass covered on one side with a thin ITO (Indium Tin Oxide) layer to form the top electrode. Very thin alignment layers were applied to both the *a*-Se and LC surface. These layers lock adjacent LC molecules in a particular orientation which causes all the molecules in the cell to align. The glass surface was then covered with spacers (3.8  $\mu\text{m}$ ) to ensure a constant gap was maintained between the glass and *a*-Se surface that contains the LC. Adhesive was applied to the perimeter of the glass surface and formed a bottleneck at one end so the LC could be inserted. The glass and selenium substrate were sandwiched together and placed in a press while the adhesive cured. This sandwiched structure was then placed in an evacuated vacuum chamber. The LC was added through the neck and filled the cell by capillary action. The neck was then sealed to contain the LC. The LC layer consisted of an ECB (electrically controlled birefringence) cell, chosen to be 3.8  $\mu\text{m}$  thick to operate in normally black mode. A linear polarizer oriented at 45° to the director (directional vector parallel to the long axis of an LC molecule) of the LC molecules was placed on the piece of glass to polarize the incoming light from the optical scanner as well as to act as an analyzer for the reflected light emerging from the XLV and incident, through optics onto the readout array.

### 2.2. Image Digitization

For image digitization, an inexpensive office scanner that is normally used to digitize images on paper was used. The scanner had an 8 bit standard output and a 16 bit internal analog to digital converter. The manufacturer's specification listed 1200 dpi as the image resolution (pixel pitch of 21  $\mu\text{m}$ ). The scanhead was located on the opposite side of the scanner glass. The scanhead consisted of a light source and a row of detector elements. The light source consisted of a light pipe illuminated with an LED to achieve uniform illumination across the row of detector elements. The detector elements consisted of CMOS sensors tiled together to form a row so that each detector element (DEL) swept out an area to create a pixel on the image as the scanhead scanned the length of the paper. The DELs and the light source were fixed on a bar that was as wide as the scanner and moved along the scanner's length. This composite scan head included all of the electronics, optical equipment and the physical scan bar. It was connected to the USB port of the readout computer. The scan head rested on a metal guide the length of the scanner, and used a stepper motor to pull itself along a toothed

rubber belt. It was kept a fixed distance from the scanner glass by way of a spacer on either side between the scan head and the glass.

For our application, the scanner was modified to permit the detection of specular reflection of light from the XLV detector. The LC side of the XLV detector was placed on the scanner glass. The light source sent light through the scanner glass where it was specularly reflected at the *a*-Se surface of the XLV and detected by a DEL defined by the CMOS sensor. By scanning the entire region of interest containing the XLV, a digital radiograph was produced.

### 3. METHODS

#### 3.1. Measurement of Optical Scanner MTF

The MTF of the optical scanner was measured using the oversampled edge technique<sup>11</sup>. An edge which is part of a spatial resolution target (Newport Corporation, NRC) was used which included bar patterns with pitches of up to 200 lp/mm. The edge image was acquired by cropping an area of a bar pattern. The edge was aligned at a small angle to the scanner DELs and scanned. The oversampled edge spread function (ESF) was then binned by distance (bin size =  $\frac{1}{4}$  readout pixel pitch) to obtain a 4X oversampled ESF. The ESF was differentiated to obtain the LSF and the MTF was taken as the modulus of the Fourier transform of the LSF. A 5-point sliding average was applied to the raw MTF data obtained from the modulus of the Fourier transform of the LSF.

#### 3.2. Determination of Characteristic Curve of XLV

It is necessary that a system exhibits linear response if linear systems analysis and metrics are used to characterize system performance. Therefore the first step in measurement is to determine linearity or, if the system is non-linear, to establish whether it can be linearized. For this purpose the *characteristic curve* of a system is required which shows the output of the system (i.e. pixel values of an x-ray image) as a function of input (x-ray exposure). Since we wish to obtain the MTF of the XLV, we first obtained the characteristic curve.

The characteristic curve of the XLV was measured experimentally to determine the response of the XLV as a function of dose. For this experiment, the XLV was biased to a normally black state (can be achieved with x-rays or an applied voltage during readout) and a series of 10 exposures were acquired at equal intervals. This was done by placing a thick lead block the width of the XLV in front of the detector so that the entire XLV was blocked from radiation. An image was acquired prior to any exposure to permit image correction which is described in the next section. The block was moved a fixed distance (a tenth of the width of the detector) with a stepper motor and the first exposure was taken. The process was repeated until all ten exposures were completed. Once all the exposures had been taken, the image was readout resulting in a step-wedge image ranging from dark (non-exposed) regions to bright (exposed) regions. The average image intensity of each step was then plotted as a function of exposure at that step – this is the experimental characteristic curve.

#### 3.3. Image Correction

Non-uniformities exist in all x-ray detectors and the XLV is no different. To correct for these non-uniformities, an image correction routine was applied to each image used for analysis. This correction routine for a single edge image is described below.

First, the detector was biased to a normally black state and an image was acquired prior to any exposure, referred to here as the *dark image*. The edge was then placed in front of the detector and an x-ray edge image was acquired. The entire XLV was then erased with white light LEDs. Once the XLV was completely erased, the edge was removed and another dark image was acquired prior to exposure. Two *dark* images were required since the x-ray exposure and XLV erasure could affect XLV response. The XLV was then exposed to achieve a *bright* state, i.e. all of the LC molecules aligned with *E*. The first dark image was subtracted from the x-ray edge image to correct for a fixed offset present before any exposure. The pixels values in the bright image were then divided by the pixel values in the second dark image to

calculate a gain matrix to account for the non-uniformities in the XLV response. The edge image was then multiplied by this gain matrix resulting in a gain and offset corrected edge image. From this edge image, the ESF and LSF were calculated and the MTF was obtained with the method described above.

### 3.4. Measurement of XLV MTF

To create the slanted edge image, the XLV device was placed in the readout scanner that was in a holder 165 cm from the focal spot of the x-ray tube. A tungsten edge measuring  $16.6 \text{ cm} \times 5.3 \text{ cm} \times 0.3 \text{ cm}$  was attached to the front of the holder at an angle of  $1.5^\circ$  relative to the readout scanner pixels such that it could be removed and repositioned accurately as needed. The edge was placed in the centre of the x-ray beam and 1 cm from the XLV detector to avoid geometric effects.

## 4. RESULTS

The characteristic curve of the XLV is shown in Figure 3. The XLV exhibited nearly linear response in the range of 0 – 10 mR. We assumed the XLV to be linear in this region and the edge images used for MTF analysis were taken in this exposure range (unexposed region = 0 mR, exposed region = 12.5 mR).

The MTF of the optical scanner is shown in Figure 4. The MTF was plotted along with the aperture response of a  $21 \mu\text{m}$  pixel in the optical scanner. The scanner MTF was lower than the sinc function of its pixel response indicating the MTF of the scanner was not limited by its pixel size but more likely the focusing of the optical components. The MTF of the XLV and optical scanner are summarized in Figure 5 and both were very high with the XLV reaching 50% past 5 cycles/mm.

From Figure 5, we can see that the MTF of the XLV system is lower than that of the optical scanner alone. The MTF of *a*-Se is very high but is not unity for all spatial frequencies shown. Also, field spreading resulting from charge collected at the *a*-Se – LC interface could result in blur in the optical image created in the LC cell. These two factors could account for the observed drop in total system MTF.

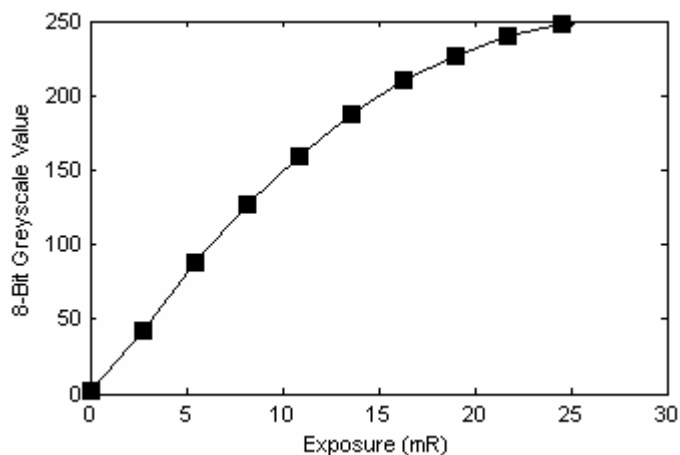


**Figure 3:** Characteristic curve of the XLV. Exposures were acquired at 2.72 mR for a total of 10 exposures. The XLV had a nearly linear response between 0 – 10 mR.

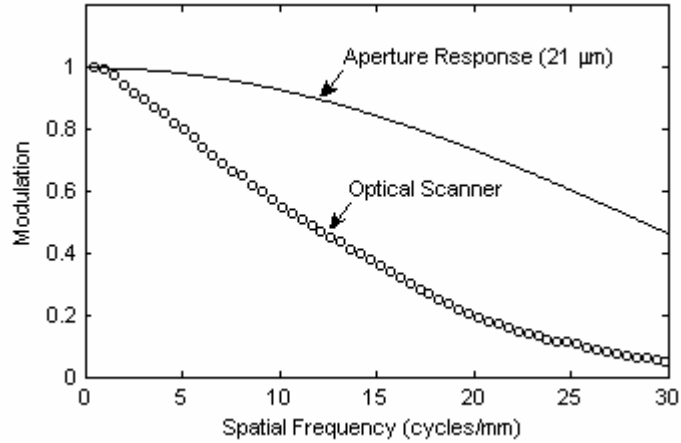


**Figure 4:** MTF of the optical scanner and aperture response for a 21  $\mu\text{m}$  pixel . The MTF of the scanner is below that of the aperture response indicating the scanner MTF was limited by the focusing optics and not the pixel size.

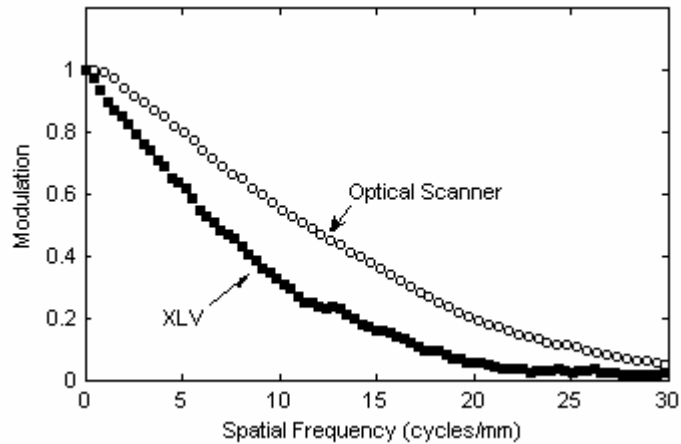


**Figure 5:** MTF of the optical scanner and entire XLV system. The MTF of the XLV was lower than that of the optical scanner for all spatial frequencies. From this graph, we can conclude that the optical scanner is the limiting factor regarding spatial resolution since the XLV MTF, which is modulated by the optical scanner MTF, was not significantly lower than that of the scanner.

## 5. DISCUSSION

In order to quantify the XLV MTF in terms of the resolution requirement for chest imaging, the inherent resolution of the XLV device alone was calculated by removing the digitization stage (i.e.  $MTF_{XLV} = MTF_{TOTAL}/MTF_{SCANNER}$ ). The resolution requirement for chest radiography is defined by a pixel size of 200  $\mu\text{m}$ . The aperture response of a 200  $\mu\text{m}$  pixel is plotted along with the resolution of the XLV detector in Figure 6. The XLV exceeds this requirement for all spatial frequencies. It is clear that an XLV system with 200  $\mu\text{m}$  pixels would be limited by the aperture response of the pixel and not the fundamental physics involved in image formation.

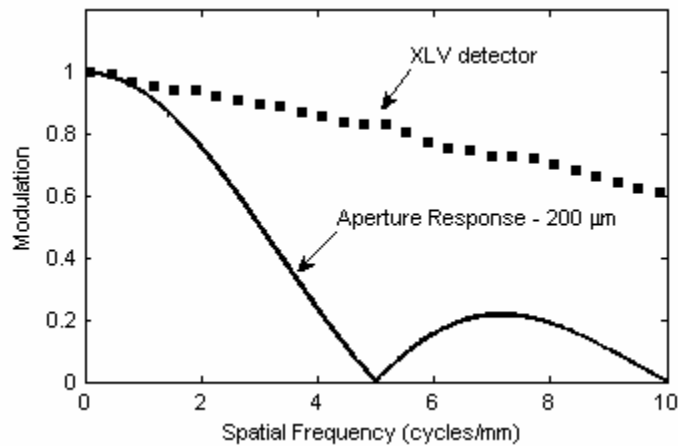


**Figure 6:** The MTF of the XLV detector (optical scanner MTF removed) and the aperture response of a 200  $\mu\text{m}$  pixel which defines the spatial resolution requirement for chest radiography. The XLV detector exceeds that of the aperture response for all spatial frequencies.

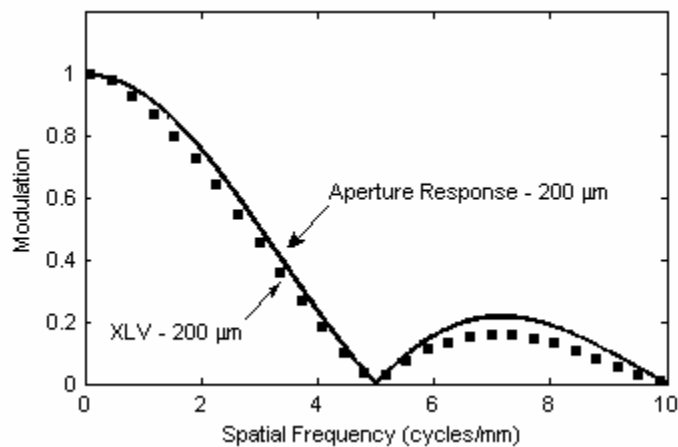


**Figure 7:** Simulated MTF of an XLV with 200  $\mu\text{m}$  pixels and the aperture response for this pixel size. The XLV follows the aperture response for all spatial frequencies indicating that for the XLV is capable of achieving the maximum resolution for this pixel size.

The simulated MTF of such an XLV with 200  $\mu\text{m}$  pixels is shown in Figure 7. The XLV MTF and the aperture response of its pixel are essentially identical over all spatial frequencies. Thus, the XLV would meet or exceed the resolution of any chest radiography imaging system with an equivalent pixel size.

## 6. CONCLUSION

The X-ray Light Valve (XLV) is a revolutionary approach to achieve a low-cost, high quality digital x-ray imaging system for chest radiography. Currently, the resolution of the XLV is limited by the optical scanner used for image digitization. Although this is the limiting factor for the current experimental system, it is not seen as a fundamental limit on resolution since a higher quality scanner could be used to increase the resolution in the digitization stage. For a

typical chest radiography system with a pixel size of 200  $\mu\text{m}$ , a scanning device could easily be made to have an MTF identical to that of the aperture response. The XLV device also has the potential to achieve the maximum possible resolution at this pixel size. Thus, we have shown that the XLV device is able to meet the resolution requirements for chest radiography.

## REFERENCES

1. J.A. Rowlands and J. Yorkston, "Flat panel detectors for digital radiography," in: *Medical Imaging. Volume 1 Physics and Psychophysics*, pp. 223-328. (SPIE, Bellingham, 2000).
2. M.J. Yaffe and J.A. Rowlands, "X-ray detectors for digital radiology", *Physics in Medicine and Biology*, **42**, 1-39 (1997).
3. J.A. Rowlands, "Physics of computed radiography", *Physics in Medicine and Biology*, **47**, R123-R166 (2002).
4. J.W. May, A.R. Lubinski, "High resolution computed radiography by scanned luminescent toner radiography", *Proc. SPIE*, **1896**, 292-312 (1993).
5. M. Bath, P. Sund and L.G. Mansson, "Evaluation of the imaging properties of two generations of a CCD-based system for digital chest radiography", *Medical Physics*, **29**, 2286-2297 (2002).
6. J.A. Rowlands, C.A. Webster, I. Koprinarov, P. Oakham, K.C. Scahd, T. Szeto, S. Germann, "Low cost digital radiographic imaging systems: The x-ray light valve", *Physics of Medical Imaging*, Proc. SPIE.
7. P.K. Rieppo, B. Bahadur, and J.A. Rowlands, "Amorphous selenium liquid crystal light valve for x-ray imaging", in R.L. Van Metter and J. Beutel, Eds., *Physics of Medical Imaging*, Proc. SPIE **2432**, 228-236.
8. P.K. Rieppo and J.A. Rowlands, "X-ray imaging using amorphous selenium: Theoretical feasibility of the liquid crystal light valve for radiography", *Medical Physics*, **24**, 1279-1292 (1997).
9. G. Hajdok, J. Yao, J.J. Battista, I.A. Cunningham, "Signal and noise transfer properties of photoelectric interactions in diagnostic x-ray imaging detectors", *Medical Physics*, **33**, 3601-3620 (2006).
10. W. Que and J.A. Rowlands, "X-ray imaging using amorphous selenium: Inherent spatial resolution", *Medical Physics*, **22**, 365-374 (1995).
11. E. Samei, M.J. Flynn, D.A. Reinmann, "A method for measuring the presampled MTF of digital radiographic systems using an edge test device", *Medical Physics*, **25**, 102-113 (1998).